Parametric Sensitivity and Uncertainty Propagation in Dependability Models

Riccardo Pinciroli
DEIB, Politecnico di Milano
Milano, 20133, Italy
riccardo.pinciroli@polimi.it

Kishor S. Trivedi
Department of ECE, Duke University
Durham, NC 27708, USA
ktrivedi@duke.edu

Andrea Bobbio
DISIT, Universita' del Piemonte Orientale
Alessandria, 15121, Italy
andrea.bobbio@uniupo.it

ABSTRACT

Input parameters of dependability models are often not known accurately. Two principal methods of dealing with such parametric uncertainty are: sensitivity analysis and uncertainty propagation. This paper is an initial attempt to link the two approaches. The case-study used here (i.e., the multi-voltage propulsion system for the Italian High Speed Railway) also enhances the model presented in [6].

Keywords

Epistemic uncertainty propagation; Parametric sensitivity analysis; Homogeneous and Non-Homogeneous Markov models; Hierarchical models; Railway system dependability

1. INTRODUCTION

Simple and accurate models are fundamental for a good system analysis. Modellers are required to consider different features of the system and to incorporate them to make the stochastic model as similar as possible to the real system. Furthermore, they are also asked to keep the model simple in order to get fast results and possibly fully symbolic solutions. In addition to modeling errors in the stochastic model (i.e., errors due to a bad representation of the system), epistemic uncertainty [26] must also be taken into consideration if good results are desired. Epistemic uncertainty is introduced into a model because of the way in which the input parameters of the model are derived (i.e., finite number of samples in measurement campaigns). Because of this uncertainty, output measures are conditional on the parameter values used.

Generally, a trade-off between simplicity of the model and other features such as accuracy and ease of deriving solutions exists. For example, when the modellers want to include dependencies using a state space approach: it is possible to model the system with a continuous time Markov chain (CTMC), but it is often impractical to solve a model with a large number of states, and the ease of deriving solutions decreases. Thus, it can be hard to model a real system trying to provide all these features together.

Uncertainty propagation analysis is used to distinguish between errors in model output due to bad modeling assumptions and low accuracy due to epistemic (parametric) uncertainty. The method consists in propagating epistemic uncertainty in the input parameters through the model, in order to compute the uncertainty in the output measures. Unfortunately, it is not always easy to study the uncertainty propagation. Indeed, for large and complex models it is often not practical to analytically or numerically computing the uncertainty. On the other side, parametric sensitivity analysis is a method that lets modeller identify the parameters for which the smallest variation most affects the model output measures. This analysis can be done also with complex models in short time. Different techniques in sensitivity function computation can be adopted in order to deal with different model types [4, 5, 11, 19, 22].

In this paper, we consider as a case study the model of a multi-voltage propulsion system proposed in [6] for the Italian High Speed Railway. We focus on two different aspects of modeling. First, we propose some enhancements to the original model, in order to show how it is possible to add some features to the model, while trying to keep it as simple as possible. The purpose of the added features is to make the model more accurate and yet easier to solve. Then, we consider accuracy of the same model with particular interest in epistemic uncertainty propagation and parametric sensitivity. This is the first step to find a relationship between these two aspects of the model in order to identify the parameters that have the greatest impact on the output measures and thus need to be known with higher accuracy.

The remainder of this paper is structured as follows. In Section 2 prior work on uncertainty propagation is discussed. In Section 3 a first description of the system is given through a reliability block diagram (RBD) and then the Markov model used in [6] is presented. Section 4 describes the improvements introduced in the original model in order to make it more accurate and yet easier to derive fully symbolic solutions. In Section 5 we study the accuracy of the input parameters of the model, looking for a relationship between parametric sensitivity and epistemic uncertainty. Finally, Section 6 concludes the paper.

2. RELATED WORK

There are two main kinds of uncertainty [29]: epistemic uncertainty that is due to lack of knowledge [8, 31] and aleatory uncertainty due to the natural variations of the

DOI:

DOI 10.4108/eai.25-10-2016.2266529

physical phenomenon [25,27]. For the purpose of this paper, we are interested in epistemic uncertainty since it can be reduced [1]. It has been studied both in stochastic simulation [2, 24, 30] and in analytic models [20, 21, 23].

Simulation optimization has been largely analyzed in order to take into consideration uncertainty propagation. For example, Yi, Xie and Zhou [30] proposed a seuqential experiment design to identify the samples that contribute the most to the percentile estimation. Song et al. [24] analyzed how indifference-zone formulation of ranking and selection – a procedure used to choose the best among a set of simulated alternatives – works with epistemic uncertainty. Authors of [2] estimated the input uncertainties that minimize the cost of data collection and comply with a given bound. For that purpose, they proposed a technique (i.e., inverse uncertainty propagation) to find the optimal input uncertainties so that the given bound on the simulation output uncertainty is satisfied.

Analytic methods for uncertainty propagation derive variance or confidence interval (exact or approximate) manipulating the closed-form solutions of the model output measures. Several papers in literature [9, 12, 17] only considered non-state-space models (simple series-parallel systems or fault tree), with a small number of input parameters. Author of [23] studied the uncertainty propagation through a multidimensional integration. Even if several analytical and numerical methods can be applied, the computation of integrals can be hard for large and complex models. Alternatively, Monte Carlo sampling methods have also been proposed to propagate the uncertainty through the model in order to compute the quantiles of the distribution of the model output. Some of them assume that the input parameters follow a given epistemic distribution [14], some others derive the epistemic distribution from a given confidence interval [20].

We wish to provide an easy and quick way to identify, through parametric sensitivity analysis, which parameter must be more carefully measured in order to get a tighter confidence interval on the output measures. For this purpose, we identify a relationship between uncertainty propagation and parametric sensitivity.

3. MODEL DESCRIPTION

The multi-voltage propulsion system, originally proposed in [6] and [7], consists of three equivalent modules in a parallel redundant configuration. In Figure 1 the RBD of the system is shown. Each module is composed of transformer (T), filter (F), inverter (I) and motor (M) in series with two parallel converters (C_1 and C_2). In [6], the component times to failure are assumed to be exponentially distributed with the failure rate values reported in Table 1. Denote by $\lambda = \lambda_T + \lambda_F + \lambda_I + \lambda_M$ the total failure rate of the series components and γ the failure rate of each parallel component. The propulsion system works until one of the three parallel modules is up, but the available power capacity (i.e., the rewards of each state, see Section 3.1) depends on the number of working modules and components.

3.1 Continuous time Markov chain

The Markov chain model for the system is reported in Figure 2. Each state represents a possible configuration of the system by means of a label that has three rows, one for each parallel module, and two columns. The first column

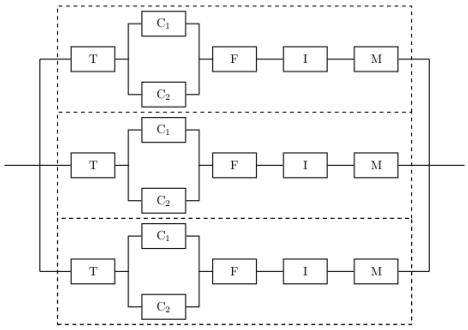

Figure 1: RBD of the propulsion system.

Table 1: System block failure rate.

Component	Failure rate [f/h]
Transformer	$\lambda_T = 2.2 \cdot 10^{-6}$
Converter	$\gamma = 2.8 \cdot 10^{-5}$
Filter	$\lambda_F = 4.0 \cdot 10^{-7}$
Inverter	$\lambda_I = 3.8 \cdot 10^{-5}$
Motor	$\lambda_M = 3.2 \cdot 10^{-5}$

of the label is 1 if all the series components in the module (row) are working, 0 otherwise. The second column of the label indicates how many parallel converters are working. If one series component or both the parallel ones are down, the module fails and the two digits of the label are set to 0. Each arc is labelled with a time-independent failure rate (no repair operations can be provided while the train is travelling) and hence we are dealing with a homogeneous CTMC. To compute the power capacity delivered by the multi-voltage propulsion system as a function of time, we assign to each state a reward rate indicating the power delivered in that state.

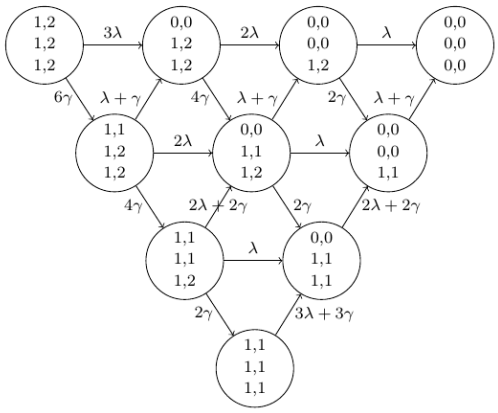

Figure 2: Original CTMC as described in [6].

Due to the state-space dimension of the CTMC of Figure 2, it is impractical to get a fully symbolic transient solution [18]. We could derive semi-symbolic or numerical solutions. Instead, in Section 4 we develop a hierarchical model that will enable us to produce a fully symbolic solution.

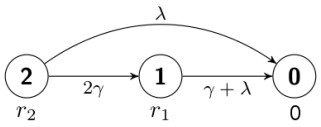

Figure 3: Markov Reward Model for one module.

4. MODEL IMPROVEMENTS

We show the steps to arrive to a fully symbolic solution while removing the constraint of constant failure rates.

4.1 Single module analysis

We start representing one single module by means of the three-state Markov reward model (MRM) shown in Figure 3. In *State 2* all the components are working, the module is fully operational and delivers a power represented by the reward rate r_2. In *State 1* only one of the two converters is operative and the module delivers a reduced power [6] represented by the reward rate r_1. *State 0* is the down state and no power is delivered. The CTMC arrives to *State 0* from *State 1* if one of the series components fails, or from *State 1* if the second converter fails.

Since the MRM has only three states, we can derive the fully symbolic transient solution, for example by resorting to Laplace transforms:

$$\begin{cases} \pi_2(t) = e^{-(2\gamma+\lambda)t} \\ \pi_1(t) = 2e^{-(\gamma+\lambda)t} - 2e^{-(2\gamma+\lambda)t} \\ \pi_0(t) = 1 - \pi_1(t) - \pi_2(t) \end{cases} \quad (1)$$

The module reliability is

$$R(t) = \pi_2(t) + \pi_1(t) = 2e^{-(\gamma+\lambda)t} - e^{-(2\gamma+\lambda)t}.$$

Denote by $X(t)$ the power delivered by the module at time t and by $Y(t)$ the energy delivered up to time t. The expected values $E[X(t)]$ and $E[Y(t)]$ of these quantities can be computed by combining the obtained state probabilities with the reward rates.

$$E[X(t)] = \sum_{i=0}^{2} r_i \pi_i(t) = r_2\pi_2(t) + r_1\pi_1(t)$$
$$= (r_2 - 2r_1)e^{-(2\gamma+\lambda)t} + 2r_1 e^{-(\gamma+\lambda)t}$$

$$E[Y(t)] = \sum_{i=0}^{2} \int_0^t r_i \pi_i(x)dx \quad (2)$$
$$= r_2 \int_0^t \pi_2(x)dx + r_1 \int_0^t \pi_1(x)dx$$
$$= \frac{(r_2 - 2r_1)(1 - e^{-(2\gamma+\lambda)t})}{2\gamma+\lambda} + \frac{2r_1(1 - e^{-(\gamma+\lambda)t})}{\gamma+\lambda}$$

Following [6], we assume $r_2 = 2200\ kW$ and $r_1 = 1100\ kW$.

The Cdf of the total energy delivered till absorption $Y(\infty)$ can be derived using the method proposed by Beaudry in [3]. The method consists in changing the domain representation of the process from a time domain to a reward domain representation, scaling the transition rates by the reward rates. Consider that in a state with reward rate r, in a time interval of length t the system accumulates a reward $y = rt$. After differentiation and manipulation we get $dt = dy/r$. Given a transition rate λ_i from a state i with reward rate r_i, the new transition rate in reward unit is λ_i/r_i as shown in Figure 4. Solving the CTMC of Figure 4, we can derive

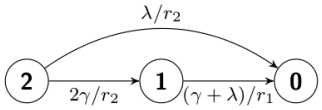

Figure 4: CTMC of the reward domain representation.

the new state probabilities in the reward domain (denoted by a superscript (R)):

$$\begin{cases} \pi_2^{(R)}(r) = e^{-\frac{(2\gamma+\lambda)}{r_2}r} \\ \pi_1^{(R)}(r) = 2r_1\gamma \cdot \dfrac{e^{-\frac{(\gamma+\lambda)}{r_1}r} - e^{-\frac{(2\gamma+\lambda)}{r_2}r}}{\gamma(2r_1 - r_2) + \lambda(r_1 - r_2)} \\ \pi_0^{(R)}(r) = 1 - \pi_1^{(R)}(r) - \pi_2^{(R)}(r) \end{cases} \quad (3)$$

and finally we compute the Cdf of the accumulated reward till absorption as:

$$Pr(Y(\infty) \geq y) = \pi_1^{(R)}(y) + \pi_2^{(R)}(y)$$
$$= \frac{[(r_1 - r_2)\lambda - r_2\gamma]e^{-\frac{2\gamma+\lambda}{r_2}y} + 2r_1\gamma e^{-\frac{\gamma+\lambda}{r_1}y}}{(2r_1 - r_2)\gamma + (r_1 - r_2)\lambda} \quad (4)$$

Figure 5 depicts $Pr(Y(\infty) \geq y)$ as a function of y.

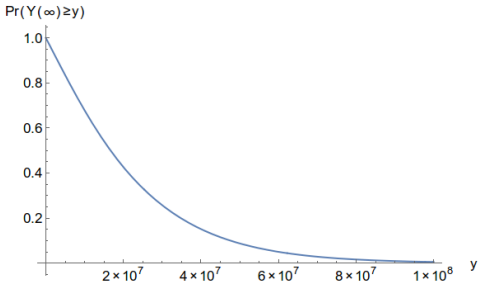

Figure 5: $Pr(Y(\infty) \geq y)$ computed as in Equation 4.

A simple algorithm to obtain the mean time to absorption in a transient CTMC is based on the computation of the expected state occupancy in the transient states before absorption. Given that τ_i is the expected state occupancy in state i and $\boldsymbol{\tau}$ the vector grouping the τ_i, we can compute the mean time to failure (MTTF), from equation [28]:

$$\boldsymbol{\tau}\boldsymbol{Q}_u = -\boldsymbol{\pi}_u(0) \quad (5)$$

where $\boldsymbol{Q}_u$ is the partition of the infinitesimal generator matrix of the CTMC over the transient states and $\boldsymbol{\pi}_u(0)$ the partition of the initial probability vector over the transient states. We compute τ_i solving (5) and then the MTTF is the sum of the τ_i over the transient states. In our case:

$$MTTF_{module} = \tau_2 + \tau_1 = \frac{1}{2\gamma+\lambda} + \frac{2\gamma}{(2\gamma+\lambda)(\gamma+\lambda)}$$
$$= \frac{3\gamma+\lambda}{(2\gamma+\lambda)(\gamma+\lambda)}$$

With the values of Table 1 $MTTF_{module} = 12104.7\,hr$. Combining expected time spent in state i before absorption, τ_i,

and the reward rate of the same state, r_i, we can compute the mean energy delivered till failure (MEDF) as:

$$MEDF_{module} = r_2\tau_2 + r_1\tau_1 = \frac{r_2}{2\gamma+\lambda} + \frac{2r_1\gamma}{(2\gamma+\lambda)(\gamma+\lambda)} = \frac{(r_2+2r_1)\gamma + r_2\lambda}{(2\gamma+\lambda)(\gamma+\lambda)}$$

With the assigned numerical values we get $MEDF_{module} = 2.18688 \cdot 10^7\ Wh$.

4.2 Non-Homogeneous CTMC

One of the weaknesses of the original model is that the failure rates are time-independent. In order to include aging phenomena of the components, all the rates should depend on time. For this purpose, the model presented in Section 4.1 is extended as shown in Figure 6 where rates are now time dependent. The underlying stochastic process is now a Non-Homogeneous CTMC (NHCTMC) and the entries of the generator matrix can vary over the same global time. The Markov property is still satisfied, but the homogeneity requirement is not satisfied. Kolmogorov differential equations [28] is used to define the transient behavior of a NHCTMC:

$$\frac{d\boldsymbol{\pi}(t)}{dt} = \boldsymbol{\pi}(t)\boldsymbol{Q}(t)$$

with $\boldsymbol{\pi}(t_0)$ the given initial state probability vector. The probability vector $\boldsymbol{\pi}(t)$ is subject to the normalization condition for any time $\sum_{i=1}^{n} \pi_i(t) = 1$ $(t \geq 0)$.

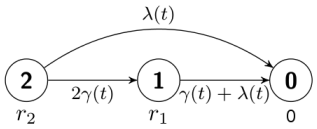

Figure 6: Markov Reward Model for one module with time dependent failure rates.

Since the NHCTMC is acyclic, we can use the *convolution integration approach* [10, 28] to derive the state probability expressions for the three states:

$$\begin{aligned}\pi_2(t) &= e^{-\int_0^t(\lambda(x)+2\gamma(x))dx} \\ &= e^{-\int_0^t \lambda(x)dx} \cdot e^{-\int_0^t 2\gamma(x)dx} = e^{-(\Lambda(t)+2\Gamma(t))}\end{aligned} \tag{6}$$

where

$$\Lambda(t) = \int_0^t \lambda(x)dx \ , \quad \Gamma(t) = \int_0^t \gamma(x)dx$$

$$\begin{aligned}\pi_1(t) &= \int_0^t \pi_2(x)\cdot 2\gamma(x)\cdot e^{-\int_x^t(\lambda(y)+\gamma(y))dy}dx \\ &= \int_0^t e^{-(\Lambda(x)+2\Gamma(x))}\cdot 2\gamma(x)\cdot e^{-\int_x^t(\lambda(y)+\gamma(y))dy}dx \\ &= 2\int_0^t e^{-\int_0^t(\lambda(y)+\gamma(y))dy}\cdot\gamma(x)\cdot e^{-\Gamma(x)}dx \\ &= 2e^{-(\Lambda(t)+\Gamma(t))}\cdot(1-e^{-\Gamma(t)}) \\ &= 2e^{-(\Lambda(t)+\Gamma(t))} - 2e^{-(\Lambda(t)+2\Gamma(t))}\end{aligned} \tag{7}$$

$$\begin{aligned}\pi_0(t) &= 1-\pi_2(t)-\pi_1(t) \\ &= 1+e^{-(\Lambda(t)+2\Gamma(t))} - 2e^{-(\Lambda(t)+\Gamma(t))}\end{aligned} \tag{8}$$

Once we have derived the state probability expressions, we can compute the expected power available at time t and the expected energy delivered in the interval $(0, t]$ using the reward rates r_1 and r_2:

$$\begin{aligned}E[X(t)] &= r_2\pi_2(t) + r_1\pi_1(t) \\ &= (r_2-2r_1)e^{-(\Lambda(t)+2\Gamma(t))} + 2r_1e^{-(\Lambda(t)+\Gamma(t))}\end{aligned}$$

$$\begin{aligned}E[Y(t)] &= r_2\int_0^t \pi_2(x)dx + r_1\int_0^t \pi_1(x)dx \\ &= r_2\int_0^t e^{-(\Lambda(x)+2\Gamma(x))}dx \\ &\quad + r_1\int_0^t 2e^{-(\Lambda(x)+\Gamma(x))} - 2e^{-(\Lambda(x)+2\Gamma(x))}dx\end{aligned} \tag{9}$$

4.3 Hierarchical model

The models described in Sections 4.1 and 4.2 still refer to one single module of the three lines of the multi-voltage propulsion system. Now we extend our argument to consider the whole system with the goal of arriving to a fully symbolic solution not easily obtained from the CTMC of Figure 2.

To build up a model for the whole system of Figure 1, we assume statistical independence among the three parallel modules, and we use a hierarchical approach whose structure is depicted in Figure 7. The highest level of the hierarchy is implemented with a multivalued Fault Tree, in which the top event is the system failure. The top event is the output of an AND gate whose inputs are the module failures. At the lower level of the hierarchy there are the NHCTMC of Figure 6 modeling the module failures. The top event occurs when all the inputs occur, i.e., all the three modules fail. Each basic event can be in one of the three states of Figure 6 and we indicate by n_i the number of modules in state i $(i = 0,\ 1,\ 2)$ where $0 \leq n_0, n_1, n_2 \leq 3$ and $n_0 + n_1 + n_2 = 3$. Hence, the state of the top event can be described by a triple $\{n_0, n_1, n_2\}$ indicating how many modules are in state 0, in state 1 and in state 2.

The probability of each possible output configuration is derived as:

$$\begin{aligned}\pi_{n_0,n_1,n_2} &= \binom{3}{n_0, n_1, n_2}\cdot[\pi_2(t)]^{n_2}\cdot[\pi_1(t)]^{n_1}\cdot[\pi_0(t)]^{n_0} \\ &= \frac{3!}{n_0!\ n_1!\ n_2!}\cdot[\pi_2(t)]^{n_2}\cdot[\pi_1(t)]^{n_1}\cdot[\pi_0(t)]^{n_0}\end{aligned} \tag{10}$$

where the $\pi_i(t)$ in the r.h.s. of Equation (10) are those derived in Equations (6), (7) and (8).

From the hierarchical model we can compute the expected power delivered at time t, the total energy supplied during the interval $(0, t]$ and the system MTTF. For the sake of simplicity, we consider time-independent transition rates in the lower level model i.e., the homogeneous CTMC of Figure 3 and we use the results of Equation (1) in Equation (10).

Thus, the expected power delivered at time t and the total

energy supplied during the interval $(0,t]$ are:

$$\begin{aligned}E[X(t)] = &\sum_{n_2=0}^{3}\sum_{n_1=0}^{3-n_2}(r_2n_2+r_1n_1)\binom{3}{3-n_1-n_2,n_1,n_2}\\ &\cdot[\pi_2(t)]^{n_2}\cdot[\pi_1(t)]^{n_1}\cdot[\pi_0(t)]^{3-n_1-n_2}\\ &= 3e^{-(2\gamma+\lambda)t}\cdot[2(e^{\gamma t}-1)r_1+r_2]\end{aligned}$$

$$\begin{aligned}E[Y(t)] = &\sum_{n_2=0}^{3}\sum_{n_1=0}^{3-n_2}(r_2n_2+r_1n_1)\binom{3}{3-n_1-n_2,n_1,n_2}\\ &\cdot\int_0^t[\pi_2(x)]^{n_2}\cdot[\pi_1(x)]^{n_1}\cdot[\pi_0(x)]^{3-n_1-n_2}dx\\ &= \frac{3e^{-(2\gamma+\lambda)t}}{(\gamma+\lambda)(2\gamma+\lambda)}\cdot\Big[(e^{(2\gamma+\lambda)t}-1)(\gamma+\lambda)r_2\\ &+2r_1[(1-2e^{\gamma t}+e^{(2\gamma+\lambda)t})\gamma+\lambda-\lambda e^{\gamma t}]\Big]\end{aligned} \quad (11)$$

To derive the MTTF, we start computing the reliability

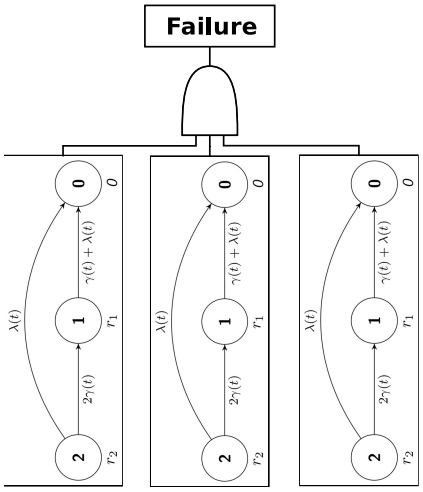

Figure 7: Hierarchical model for the multi-voltage system.

of the whole system represented by the model in Figure 7. Given the system configuration, the reliability can be derived from the equation $R_{sys}(t) = 1 - \pi_{3,0,0}$, where $\pi_{3,0,0}$ is the down state and is computed from Equation (10). In this case, the reliability is:

$$\begin{aligned}R_{sys}(t) &= 1-[1-2e^{-(\gamma+\lambda)t}+e^{-(2\gamma+\lambda)t}]^3\\ &= 12e^{-(3\gamma+2\lambda)t}+6e^{-(5\gamma+3\lambda)t}-12e^{-(4\gamma+3\lambda)t}\\ &\quad -3e^{-(2\gamma+\lambda)t}-3e^{-2(2\gamma+\lambda)t}-e^{-3(2\gamma+\lambda)t}\\ &\quad +6e^{-(\gamma+\lambda)t}-12e^{-2(\gamma+\lambda)t}+8e^{-3(\gamma+\lambda)t}\end{aligned} \quad (12)$$

Due to the simplicity of this model, same result could have been obtained by a direct application of the series/parallel reduction rules to the RBD of Figure 1. MTTF of the whole system is computed integrating the reliability as follows:

$$\begin{aligned}MTTF &= \int_0^\infty R_{sys}(t)dt\\ &= \frac{8}{3(\gamma+\lambda)}-\frac{29}{6(2\gamma+\lambda)}+\frac{12}{(3\gamma+2\lambda)}\\ &\quad -\frac{12}{(4\gamma+3\lambda)}+\frac{6}{(5\gamma+3\lambda)}\end{aligned} \quad (13)$$

Substituting the numerical values given in Table 1 to λ and γ, we obtain $MTTF = 21662.9$ hours.

5. ACCURACY ANALYSIS

In this section we study how to evaluate the accuracy of the results and how to find a convenient strategy to improve the accuracy. For this purpose, we first investigate the parametric sensitivity to identify the most affecting parameters for a chosen significant measure (the MTTF in our case), then we study how the uncertainty in the knowledge of the input parameters is propagated to the output measures. Finally, we investigate a possible relation between sensitivity and uncertainty.

5.1 Parametric sensitivity

Parametric sensitivity is a technique used to identify components that most affect an output measure. In this paper we focus on the MTTF whose expression, for the system with time-independent failure rates, is given in Equation (13).

Differential analysis [13, 19] is the basis of many sensitivity analysis techniques. The sensitivity $S_\theta(MTTF)$ of the MTTF with respect to the model parameter θ is obtained by computing the partial derivative of the metric of interest with respect to the parameter, as in Equation (14):

$$S_\theta(MTTF) = \frac{\partial MTTF}{\partial\theta}, \quad \theta = \{\lambda_T, \lambda_F, \lambda_I, \lambda_M, \gamma\} \quad (14)$$

The dimensionless scaled sensitivity is defined as follows [11]:

$$SS_\theta(MTTF) = \frac{\partial MTTF}{\partial\theta}\cdot\frac{\theta}{MTTF} \quad (15)$$

Adoption of scaled or unscaled sensitivity depends on several factors: type of the output metrics; the range of values of the output and input parameters; etc. In this paper we use the scaled sensitivity as computed in Equation (15). For one of the series components with rate λ_X with $X = \{T, I, F, M\}$, the scaled sensitivity in Equation (15) becomes:

$$SS_{\lambda_X}(MTTF) = -\lambda_X\cdot\frac{\frac{8}{3(\gamma+\lambda)^2}-\frac{29}{6(2\gamma+\lambda)^2}+\frac{24}{(3\gamma+2\lambda)^2}-\frac{36}{(4\gamma+3\lambda)^2}+\frac{18}{(5\gamma+3\lambda)^2}}{\frac{8}{3(\gamma+\lambda)}-\frac{29}{6(2\gamma+\lambda)}+\frac{12}{3\gamma+2\lambda}-\frac{12}{4\gamma+3\lambda}+\frac{6}{5\gamma+3\lambda}} \quad (16)$$

Expanding Equation (15) for a parallel converter with failure rate γ, we obtain:

$$SS_\gamma(MTTF) = -\gamma\cdot\frac{\frac{8}{3(\gamma+\lambda)^2}-\frac{29}{3(2\gamma+\lambda)^2}+\frac{36}{(3\gamma+2\lambda)^2}-\frac{48}{(4\gamma+3\lambda)^2}+\frac{30}{(5\gamma+3\lambda)^2}}{\frac{8}{3(\gamma+\lambda)}-\frac{29}{6(2\gamma+\lambda)}+\frac{12}{3\gamma+2\lambda}-\frac{12}{4\gamma+3\lambda}+\frac{6}{5\gamma+3\lambda}} \quad (17)$$

In Table 2, numerical values of the scaled sensitivity of MTTF computed through Equations (16) and (17) are reported. They have been sorted from the most to the least

sensitive. Note that all the values are negative meaning that if the value of the parameter θ increases, the MTTF decreases. The most influential component in affecting the MTTF is the inverter which is the component with the largest failure rate value.

Figure 8 shows the variation of the MTTF as a function of the variation of the failure rate of one single component, keeping all the other failure rates constant. The larger is the parametric sensitivity in absolute value, as reported in Table 2, the greater is the benefit that is possible to obtain if the considered component failure rate is improved. The straight line in Figure 8 is the current value of MTTF, as computed with Equation (13).

Table 2: Ranking based on scaled sensitivities of MTTF.

θ	$SS_\theta(MTTF)$
λ_I	$-4.16997 \cdot 10^{-1}$
λ_M	$-3.51155 \cdot 10^{-1}$
γ	$-2.03316 \cdot 10^{-1}$
λ_T	$-2.41419 \cdot 10^{-2}$
λ_F	$-4.38944 \cdot 10^{-3}$

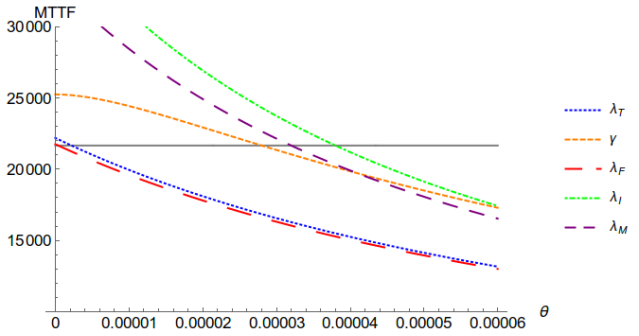

Figure 8: MTTF of the system computed varying the failure rate of one component at a time. Each curve is obtained varying the considered parameter between 0 and $6 \cdot 10^{-5}$, and keeping constant all the other failure rates. The straight line is the current value of MTTF, as computed from Equation (13).

5.2 Uncertainty propagation

We derive the uncertainty propagation through the analytic closed-form approach described in [20, 21], then we compare the results with those obtained from the parametric sensitivity analysis of Section 5.1.

Input parameters of a model have uncertainty associated with them (called epistemic uncertainty [26]), since they are derived from a finite number of observations in measurement campaigns. Authors of [21] describe a closed-form approach to compute how the uncertainty in the model input parameters propagates to the model output affecting the reliability of the system. The same procedure can be applied to compute the uncertainty propagation for other output measures, like the MTTF considered in this paper. Let the input parameters of the model be the random variables $(\Lambda_1, \Lambda_2, \ldots, \Lambda_\ell)$. The MTTF can be viewed as a random function of the ℓ input parameters $MTTF(\Lambda_1, \Lambda_2, \ldots, \Lambda_\ell)$ indicated, for short, as $MTTF(\bullet)$. The technique derived from [20, 21] consists in computing the unconditional expected MTTF through the following equation:

$$E[MTTF] = \int \ldots \int MTTF(\bullet) f(\bullet) d\lambda_1 \ldots d\lambda_\ell \qquad (18)$$

where the input parameters are set to $\Lambda_1 = \lambda_1$, $\Lambda_2 = \lambda_2$, ..., $\Lambda_\ell = \lambda_\ell$ and $f(\bullet)$ is the joint epistemic density $f_{\Lambda_1, \Lambda_2, \ldots, \Lambda_\ell}(\lambda_1, \lambda_2, ..., \lambda_\ell)$ of the input parameters

Let X be an exponentially distributed random variable of rate Λ and let $f_\Lambda(\lambda)$ be the prior density of Λ. We observe a sample of k independent and identically distributed (iid) random realizations of X, say $X_1, X_2, ..., X_k$. Setting $S = \sum_{i=1}^{k} X_i$, the conditional density of Λ given $S = s$ can be derived from the continuous version of Bayes's theorem and it is shown to be [21] a k-stage Erlang distribution with parameter s:

$$f_{\Lambda|S}(\lambda|s) = \frac{\lambda^{k-1} s^k e^{-\lambda s}}{(k-1)!} \qquad (19)$$

Since we are considering exponentially distributed time to failures, the maximum likelihood estimate for the rate λ in Equation (19) is $\hat{\lambda} = k/s$. In this setting, the unconditional expected MTTF is computed from:

$$E[MTTF] = \int_0^\infty \int_0^\infty \int_0^\infty \int_0^\infty \int_0^\infty MTTF(\bullet) \cdot \prod_\theta \frac{\theta^{k_\theta - 1} {s_\theta}^{k_\theta} e^{-\theta s_\theta}}{(k_\theta - 1)!} \, d\theta \qquad (20)$$

where $\theta = \{\lambda_T, \gamma, \lambda_I, \lambda_F, \lambda_M\}$ and k_θ and s_θ are the values of k and s computed for the component with rate θ. In Equation (20) we can define the joint pdf $f(\bullet)$ as a product of the marginal pdfs since we assume that the model input parameters are independent random variables.

Figure 9a shows $E[MTTF]$ of the considered system computed from (20) as a function of the sample size k. The dashed line at the bottom of the graph is the MTTF computed with the parameter values of Table 1, to which the expected MTTF tends asymptotically as $k_\theta \to \infty$. Note that, for simplicity, the value of k_θ is kept the same for all the parameters.

The variance of the MTTF can be computed from

$$Var[MTTF] = E[MTTF^2] - (E[MTTF])^2 \qquad (21)$$

and is depicted in Figure 9b. In this case, for $k_\theta \to \infty$ the variance tends to zero. The smaller is the variance, the tighter will be the confidence interval of the considered output measure.

With equation:

$$E[MTTF] = \int_0^\infty MTTF \frac{\theta^{k_\theta - 1} s_\theta^{k_\theta} e^{-\theta s_\theta}}{(k_\theta - 1)!} d\theta \qquad (22)$$

it is possible to evaluate the uncertainty introduced in the MTTF by the single parameter θ, while all the other parameters are assumed to have the constant value of Table 1. Variance can still be derived through Equation (21). Results are depicted in Figure 10. Each curve represents the $E[MTTF]$ ($Var[MTTF]$) of the system that is computed through Equation (22) for the considered parameter. For $k \to \infty$ the expected MTTF tends to the MTTF computed with the parameters of Table 1, whereas the variance tends to zero.

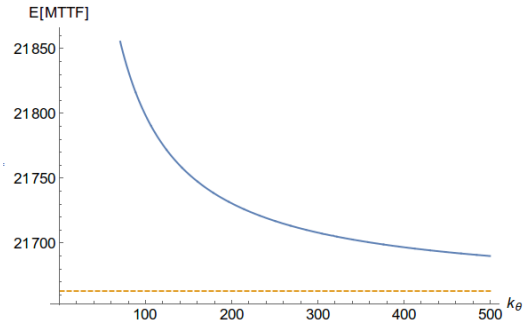

(a)

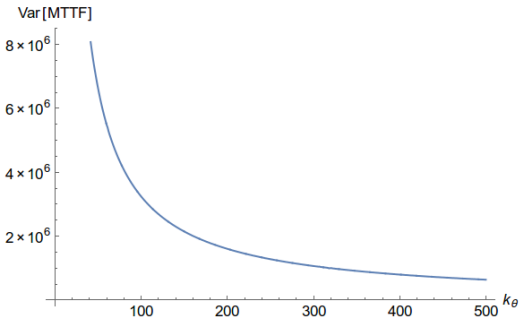

(b)

Figure 9: Expected value (a) and variance (b) of MTTF of the multi-voltage propulsion system.

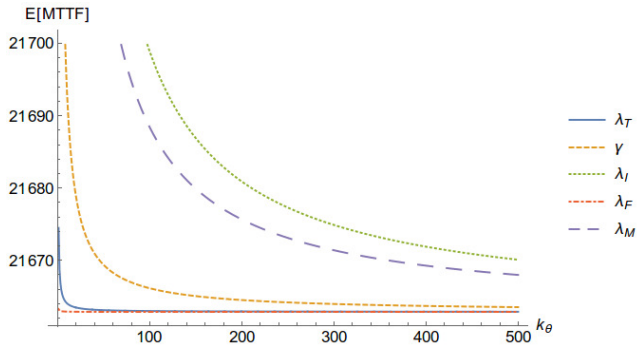

(a)

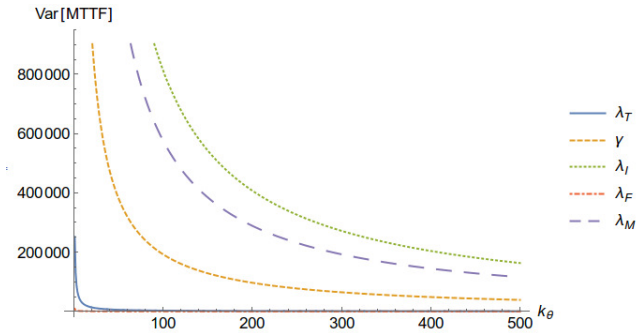

(b)

Figure 10: Expected value (a) and variance (b) of the MTTF varying the estimated parameter.

5.3 Sensitivity vs. Uncertainty Propagation

The closed-form approach to the uncertainty propagation requires the computation of a multiple integral for each parameter; symbolic or numerical computation of such integral becomes impractical for complex and large models [20]. Moreover, this technique also requires us to specify the joint epistemic density of all the parameters: this step may be difficult even if it can be simplified considering independent parameters (as we have done in this paper).

From Table 2 and Figure 10 it is possible to observe that for the parameters with a larger absolute value of the sensitivity a larger number of samples is needed to reach the same tight confidence interval. Results obtained in Sections 5.1 and 5.2 show that a relationship between parametric sensitivity and uncertainty propagation exists. Parametric sensitivity evaluation through partial derivatives is easier and quicker to carry out than uncertainty propagation through integral computation. The same observation remains valid for other parametric sensitivity computation methods, such as percentage difference [15] and Design of Experiments [16].

The above mentioned relationship allows us to use parametric sensitivity analysis to identify the parameters that need tighter confidence interval to get more accurate output measures. This method is less affected by the largeness and complexity of the system than the uncertainty propagation technique.

6. CONCLUSIONS

The multi-voltage propulsion system proposed in [6] and developed for the Italian High Speed Railway is the case study analyzed in this paper. Some techniques to simplify the derivation of fully symbolic solution and to get more accurate results are presented. In the considered case study, it is possible to model the whole system with a hierarchical model to obtain a symbolic solution for the model measures like the reliability and the MTTF. In addition, adopting a MRM it is possible to evaluate measures related to the delivered power. Further, time dependent failure rates can be included in the model by still deriving a symbolic solution.

In this paper, parametric sensitivity and epistemic uncertainty of the input parameters are also considered. A relevant result shows that a relationship between these two evaluation methods exists. It means that, for more complex models it is possible to use the parametric sensitivity analysis instead of the uncertainty propagation to identify the parameters that need a larger number of samples to reach the same accuracy. Note, however, that the same method cannot predict how many samples are needed to attain a given level of accuracy because the parametric sensitivity does not depend on the number of samples.

This paper is the first attempt to find a relationship between parametric sensitivity and uncertainty propagation. We wish to formalize this relationship and investigate possible generalizations. Two different ways can be envisaged to extend the paper in this direction: to analyze other output measures (e.g, reliability, availability, etc.) and to consider different applications. A more challenging direction of our research is toward building an optimization problem. Indeed, since a larger number of observations entails increased costs for the measurement campaign, a trade-off between cost and accuracy of the output measures exists and can be analyzed.

Acknowledgement

This research was supported in part under US NSF grant number CNS-1523994, by US Navy under grant N00174-16-C-0036, by IBM under a faculty grant, by NATO under Science for Peace project number 984425 and by DiSit-UniUpo local research Project.

7. REFERENCES

[1] H. R. Bae, R. V. Grandhi, and R. A. Canfield. Epistemic uncertainty quantification techniques including evidence theory for large-scale structures. *Computers & Structures*, 82(13–14):1101–1112, 2004.

[2] P. Baumgärtel, G. Endler, A. M. Wahl, and R. Lenz. Inverse uncertainty propagation for demand driven data acquisition. In *Proceedings of the 2014 Winter Simulation Conference*, pages 710–721. IEEE, 2014.

[3] M. D. Beaudry. Performance-related reliability measures for computing systems. *Computers, IEEE Transactions on*, 100(6):540–547, 1978.

[4] J. T. Blake, A. L. Reibman, and K. S. Trivedi. Sensitivity analysis of reliability and performability measures for multiprocessor systems. *ACM SIGMETRICS Performance Evaluation Review*, 16(1):177–186, 1988.

[5] A. Bobbio and A. Premoli. Fast algorithm for unavailability and sensitivity analysis of series-parallel systems. *IEEE Transactions on Reliability*, R-31:359–361, 1982.

[6] G. Cosulich, P. Firpo, and S. Savio. Power electronics reliability impact on service dependability for railway systems: a real case study. In *Industrial Electronics, 1996. ISIE'96., Proceedings of the IEEE International Symposium on*, volume 2, pages 996–1001. IEEE, 1996.

[7] G. Dazi, S. Savio, and P. Firpo. Estimate of components reliability and maintenance strategies impact on trains delay. In *Proc 21st European Conf on Modelling and Simulation ECMS*, 2007.

[8] A. De Galizia, C. Simon, P. Weber, B. Iung, C. Duval, and E. Serdet. Modelling non-deterministic causal mechanisms involving resilience in risk analysis. In *8th IFAC Conference on Manufacturing, Management & Control, MIM 2016*, 2016.

[9] R. G. Easterling. Approximate confidence limits for system reliability. *Journal of the American Statistical Association*, 67(337):220–222, 1972.

[10] T. E. Fortmann and K. L. Hitz. *An introduction to linear control systems*. Crc Press, 1977.

[11] R. Fricks and K. Trivedi. Importance analysis with markov chains. In *Proceedings IEEE Annual Reliability and Maintainability Symposium*, pages 89–95, 2003.

[12] M. A. S. Guth. A probabilistic foundation for vagueness and imprecision in fault-tree analysis. *IEEE Transactions on Reliability*, 40(5):563–571, Dec 1991.

[13] D. Hamby. A review of techniques for parameter sensitivity analysis of environmental models. *Environmental monitoring and assessment*, 32(2):135–154, 1994.

[14] B. R. Haverkort and A. M. Meeuwissen. Sensitivity and uncertainty analysis of markov-reward models. *IEEE Trans Reliability,*, 44(1):147–154, 1995.

[15] F. Hoffman and R. Gardner. Evaluation of uncertainties in radiological assessment models. In *Radiological Assessment: A Textbook on Environmental Dose Analysis*, pages 11.1–11.55. United States Nuclear Regulatory Commission Washington, DC, 1983.

[16] R. Jain. *The art of computer systems performance analysis*. John Wiley & Sons, 2008.

[17] G. Lieberman and S. Ross. Confidence intervals for independent exponential series systems. *J American Statistical Association*, 66(336):837–840, 1971.

[18] R. A. Maire, A. L. Reibman, and K. S. Trivedi. Transient analysis of acyclic markov chains. *Performance Evaluation*, 7(3):175–194, 1987.

[19] R. Matos, J. Araujo, D. Oliveira, P. Maciel, and K. Trivedi. Sensitivity analysis of a hierarchical model of mobile cloud computing. *Simulation Modelling Practice and Theory*, 50:151–164, 2015.

[20] K. Mishra, K. Trivedi, and R. Some. Uncertainty analysis of the remote exploration and experimentation system. *J. of Spacecraft and Rockets*, 49(6):1032–1042, 2012.

[21] K. Mishra and K. S. Trivedi. Closed-form approach for epistemic uncertainty propagation in analytic models. In *Stochastic Reliability and Maintenance Modeling*, pages 315–332. Springer, 2013.

[22] J. K. Muppala and K. S. Trivedi. Gspm models: sensitivity analysis and applications. In *Proc 28th Ann Southeast Regional Conf*, pages 25–33. ACM, 1990.

[23] N. D. Singpurwalla. *Reliability and risk: a Bayesian perspective*. John Wiley & Sons, 2006.

[24] E. Song, B. L. Nelson, and L. J. Hong. Input uncertainty and indifference-zone ranking & selection. In *Proceedings of the 2015 Winter Simulation Conference*, pages 414–424. IEEE, 2015.

[25] O. Strack, R. Leavy, and R. M. Brannon. Aleatory uncertainty and scale effects in computational damage models for failure and fragmentation. *International Journal for Numerical Methods in Engineering*, 102(3-4):468–495, 2015.

[26] L. Swiler, T. Paez, and R. Mayes. Epistemic uncertainty quantification tutorial. In *Proceedings of the IMAC-XXVII*. Society for Experimental Mechanics Inc., 2009.

[27] D. Tannenbaum, C. R. Fox, and G. Ülkümen. Judgment extremity and accuracy under epistemic vs. aleatory uncertainty. *Management Science*, 2016.

[28] K. S. Trivedi. *Probability & statistics with reliability, queuing and computer science applications*. John Wiley & Sons, 2008.

[29] R. L. Winkler. Treatment of aleatory and epistemic uncertainty uncertainty in probabilistic risk assessment. *Reliability Engineering & System Safety*, 54(2):127–132, 1996.

[30] Y. Yi, W. Xie, and E. Zhou. A sequential experiment design for input uncertainty quantification in stochastic simulation. In *Proc. of the 2015 Winter Simulation Conference*, pages 447–458. IEEE, 2015.

[31] K. Zwirglmaier and D. Straub. A discretization procedure for rare events in bayesian networks. *Reliability Engineering & System Safety*, 153:96–109, 2016.